Space debris laser ranging with a 60 W single-frequency slab nanosecond green laser at 200 Hz

Haifeng Zhang (张海峰)[1,2], Mingliang Long (龙明亮)[1,*], Huarong Deng (邓华荣)[1], Zhibo Wu (吴志波)[1,2], Zhien Cheng (程志恩)[1], and Zhongping Zhang (张忠萍)[1,2]

[1]*Shanghai Astronomical Observatory, Chinese Academy of Sciences, Shanghai 200030, China*
[2]*Key Laboratory of Space Object and Debris Observation, Chinese Academy of Sciences, Nanjing 210008, China*
**Corresponding author: F_CEO_beifeng@126.com*

Received November 15, 2018; accepted March 1, 2019; posted online May 17, 2019

Space debris laser ranging was achieved with a 60 W, 200 Hz, 532 nm nanosecond slab, single-frequency green laser at the Shanghai Astronomical Observatory's 60 cm satellite laser ranging system. There were 174 passes of space debris measured in 2017, with the minimum radar cross section (RCS) being 0.25 m^2 and the highest ranging precision up to 13.6 cm. The RCS of space debris measured with the farthest distances in 174 passes was analyzed. The results show that the farthest measurement distance (R) and RCS (S) were fitted to $R = 1388.159S^{0.24312}$, indicating that this laser can measure the distance of 1388.159 km at an RCS of 1 m^2, which is very helpful to surveillance and research on low-Earth-orbit space debris.

OCIS codes: 140.3580, 350.1270, 140.3580.
doi: 10.3788/COL201917.051404.

Satellites have played a very important role in improving human life since the first one was launched into space in 1957. More than 5500 launches have put over 6000 satellites into space, among which less than 1000 are in working condition today[1]. As humans continue to launch large numbers of satellites into space regularly, orbital resources around the Earth will be increasingly reduced. In addition, increasingly more orbital debris is generated, which not only occupies the orbital resources, but also causes a serious threat to future and already existing space missions because of potential space collisions[2–5]. Thousands of pieces of damaging debris were produced from the well-known collision between Iridium 33 and Cosmos 2251 in 2009[2,3], and 1307 fragments were catalogued in the 168 days since this collision. Recently, the passive Russian ball lens in the space (BLITS) nano-satellite was reportedly struck by a piece of space debris. In a near-circular orbit with a perigee of 818 km, BLITS is in a crowded region of the low-Earth-orbit (LEO) environment[4]. Currently, there are approximately 25,000 pieces of debris larger than the size of balls orbiting the Earth and 500,000 pieces the size of marbles. In addition, the existing orbital debris population is self-propagating, and its density will continue to increase through random debris inter-collisions as well as human space activities. Therefore, it is urgent to track and catalog space debris, as well as to remove as much as possible.

However, the high-precision measurement of space debris is currently a problem to be solved on behalf of the global space community. The most effective debris removal and mitigation methods would be much easier to realize if the debris-objects orbital characteristics were known more precisely[6,7]. Laser ranging with avalanche diodes working in the Geiger mode, which has characteristics of high sensitivity and high gain, and being detected at the single-photon level, is one of the feasible ways to realize high-precision measurement, with the potential of accuracy one order higher in precision than that of either optical or radar tracking. In general, a selection of satellites have a laser retro-reflector on board for satellite laser ranging (SLR)[8,9]. However, it is rare to have laser retro-reflectors on space debris; thus, lasers reflected from debris are practically diffusive, which makes space debris laser ranging a more difficult task than SLR. Currently, there are only a few SLR stations that have realized space debris laser ranging. In addition, Poland achieved its first, to the best of our knowledge, laser measurements of space debris with a 10 Hz repetition rate, pulse width of 3–5 ns, and pulse energy of 450 mJ for a green (532-nm) laser in 2018[10]. Moreover, a space debris orbit prediction (OP) accuracy of 10–20 arcsec for 24–48 h can be achieved from a single laser ranging station's space debris data[4].

In recent years, the nanosecond laser was the main light source for space debris laser ranging. A 532 nm neodymium-doped yttrium aluminum garnet (Nd:YAG) laser with a pulse repetition frequency (PRF) of 1 kHz, pulse width of 10 ns, and pulse energy of 25 mJ has been applied for space debris laser ranging at the Graz SLR station. Debris objects with a radar cross-section (RCS) ranging from >15 m^2 down to <0.3 m^2 were measured successfully from more than 2500 km away, and their ranging root-mean-square (RMS) errors were approximately 0.7 m[11]. Workers at the Shanghai Astronomical Observatory (SAO) SLR station measured space debris at distances between 500 and 2200 km, with an RCS as small as 0.5 m^2 and a ranging RMS of <1 m for debris of small RCSs. The laser used had an average power greater than 60 W in a 532 nm nanosecond laser system with a PRF of 200 Hz[12]. However, most space debris is very small, and that requires a nanosecond laser of much

higher energy. Such a nanosecond green laser has been difficult to obtain in terms of the optical element, heat effect, and frequency-doubling efficiency. In recent years, a single frequency and a conduction cooling method in slab lasers have been widely used to obtain high-power and large-energy nanosecond green lasers[13–16]. In addition, a 61% conversion efficiency has been obtained when 2.9 mJ of green light is produced at a single-frequency 1064 nm input energy of 4.7 mJ[13]. In 2010, a modified ramp-fire technique was used to achieve reliable single-frequency oscillation by researchers at the Shanghai Institute of Optics and Fine Mechanics, who obtained a single energy of 10 mJ with a pulse width of 13 ns at a pulse repetition rate of 250 Hz at 1064 nm[14]. Several years later, the same group used a conductively cooled Nd:YAG zig-zag slab laser with a bounce-pumped architecture to obtain single-pulse energies of over 800 mJ at 1064 nm and 400 mJ at 532 nm with a 12.6 ns pulse width at 250 Hz; the optical-to-optical conversion efficiency reached up to 19% (808–1064 nm)[15]. Later, a 60 W single-frequency slab nanosecond green laser at 200 Hz was delivered by the Shanghai Institute of Optics and Fine Mechanics to SAO and was applied to space debris laser ranging. This laser has single-pulse energies of 600 mJ at 1064 nm and 300 mJ at 532 nm, with a pulse width of 5 ns. Moreover, a pulse energy of 62 mJ for blue laser pulses at 486.1 nm was obtained with pump energy of 190 mJ at 355 nm by a high pulse energy single-frequency hybrid 1064 nm master oscillator power amplifier, corresponding to conversion efficiency of 32.6%[16].

The proposed space debris laser ranging system described in this Letter was established based on the aforementioned SAO SLR system. It includes OP, a control system, laser system, laser transmitting system, telescope tracking mount system, high-precision timing system, and a return detection receiving system[12,16,17].

The 60 W nanosecond single-frequency slab green laser is composed of a seed injection (part I), pre-amplification (part II), a main amplifier (part III), and frequency doubling (part IV), as shown in Fig. 1. There are three Nd:YAG slab amplification stages in the main amplifier. Combined with finite-element optimization simulation, the slab amplifier heat-dissipation structure is designed reasonably with the conduction cooling method, and it realizes the effective heat dissipation of the slab laser pumping laser diode and laser slab crystal. ANSYS software was used to qualitatively analyze the feasibility of the waterway. The amplification module performs flow- and temperature-field analysis to obtain the flow rate and the pressure and temperature distribution of the internal water channel. Part I, seed injection to obtain a single-frequency seed laser, is described in detail in Ref. [14]; parts III and IV are described in detail in Ref. [15]. Finally, single-pulse energy of 300 mJ at 532 nm was achieved with a LiB_3O_5 crystal; the pulse width was 5 ns [Fig. 2(a)], the beam quality M^2 was approximately 3 [Fig. 2(b)], and the divergence angle was approximately 0.6 mrad with a beam diameter of 6 mm.

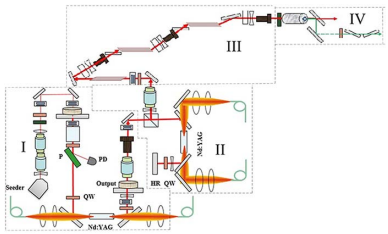

Fig. 1. 60 W nanosecond single-frequency slab green laser (for detailed information, see Refs. [12,13]).

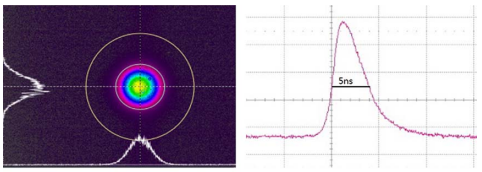

Fig. 2. a, Beam quality and, b, pulse width for 60 W nanosecond single-frequency slab green laser.

According to the laser ranging radar link equation, the parameters of the measuring system, and the RCS of space targets, the number of laser echo photons can be estimated in theory, which can provide the reference for the actual laser measurement[12,17,18]. The laser link equation is expressed as

$$n_0 = \frac{\lambda \eta_q}{hc} \times \frac{E_t A_r \rho S \cos\theta}{\pi \theta_t^2 R^4} \times T^2 \times \eta_t \times \eta_r \times \alpha, \quad (1)$$

where n_0 is the average number of photoelectrons produced by the photo-detector, λ is the laser wavelength (532 nm), η_q is the quantum efficiency of the photo-detector at the wavelength of 532 nm, E_t is the single-pulse energy, A_r is the effective receiving area of the telescope, S is the RCS of a space target, and ρ is the reflection of the space debris. Supposing that the targets are spherical, $\cos\theta = 1$. h is Planck's constant, $h = 6.6260693 \times 10^{-34}$ J · s, and c is the speed of light, $c = 3 \times 10^8$ m/s. θ_t is the divergence of the laser beam, R is the distance from the ground station to the space target, T is the atmosphere in one-way transparency, η_t is the efficiency of the transmitting optics, η_r is the efficiency of the receiving optics, and α is an attenuation factor. In this Letter, $T = 0.6$, $\eta_q = 0.4$, $E_t = 0.0016$, $A_r = 0.251$, $\eta_t = 0.6$, $\eta_r = 0.6$, $\alpha = 0.39$, and $\theta_t = 33$ μrad with three- and six-beam expanding telescopes [$(0.6/3)/6 = 0.033$ mrad]. When the reflection of the space debris ρ was 0.2, $R = 1000$ km, $S = 1\,\mathrm{m}^2$, and the number of return photons $n_0 = 0.675$.

The detection of photoelectrons follows the Poisson statistics. The probability of detecting a single photoelectron is given by the following equation[17,18]:

$$P = 1 - e^{-n_0}. \tag{2}$$

Thus, the single-pulse probability of debris detection is 48.8% for space debris with an RCS of 1 m^2 at a distance of 1000 km. We can also find from Eq. (1) that

$$R = \left(\frac{\lambda\eta_q}{hc} \times \frac{E_t A_r \rho S \cos\theta}{\pi\theta_t^2 n_0} \times T^2 \times \eta_t \times \eta_r \times \alpha\right)^{0.25} S^{0.25}. \tag{3}$$

Therefore, the ranging distance of space debris is a power function of the size of the space debris, if the space debris is detected at the same level.

The debris OPs were generated from the use of two-line element (TLE) datasets available from http://www.Space-Track.org/, with range errors at hundreds to thousands of meters. The debris names can be found at http://www.calsky.com/cs.cgi/Satellite/. With the above configuration of the proposed SLR system, the space debris was measured. Figure 3 shows the RCS values of space debris detected in 2017 from a total of 174 passes to detect space debris.

The range precision varies with the RCS of space debris, as shown in Fig. 4(a), which also shows that small pieces of space debris can be measured with high-range precision. However, larger pieces of space debris can also be measured with high-range precision. Figure 4(b) shows the range change with the RCS of space debris. It can be seen from the figure that the smaller the RCS of space debris, the shorter the range. Overall, the smallest RCS was approximately 0.25 m^2 from the debris designated ID37831 [Fig. 5(a)] and named "NOAA 12 Debris," with an orbit of 746.1 × 755.7 km, an orbital period of 99.8 min, and an inclination of 98.5°. The ranging precision was up to 13.68 cm for ID04657 [Fig. 5(b)], named "Nimb 4 Rocket DbAR Debris," with an orbit of 987.1 × 1012 km, an orbital period of 105.1 min, and an inclination of 100.1°. All of the passes did not include the space debris of Envisat, which has a laser retro-reflector array (RRA) panel for SLR that has a hemispherical shape (20 cm in diameter) and consists of nine corner cube reflectors[19].

From Fig. 4(b), the farthest measurement range with different RCS values was chosen, and the results are shown in Fig. 6. Using power-function processing, the following fitting function was obtained for the points

$$y = 1388.159x^{0.243}, \tag{4}$$

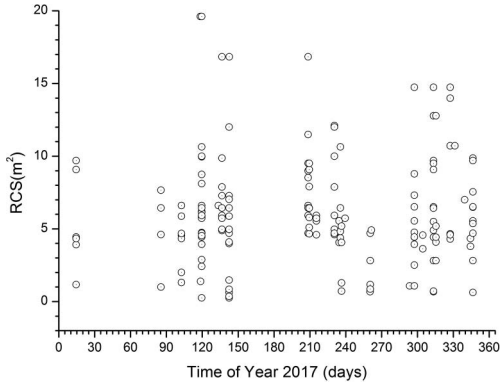

Fig. 3. Space debris detected in 2017.

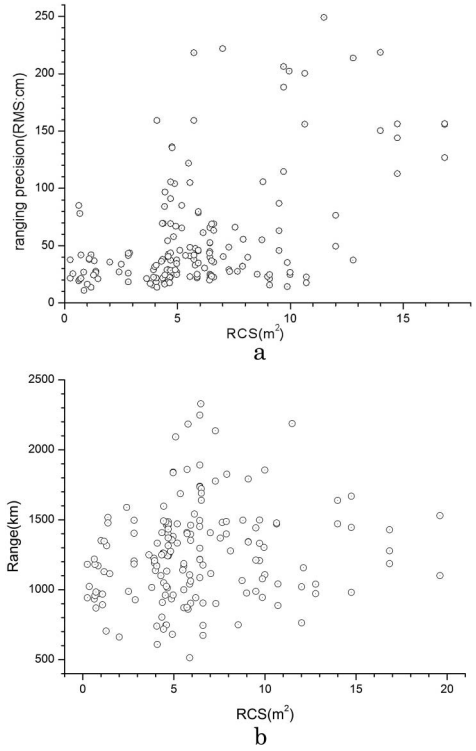

Fig. 4. Space debris laser ranging: a, range precision change with RCS and, b, range precision change with the size RCS of space debris.

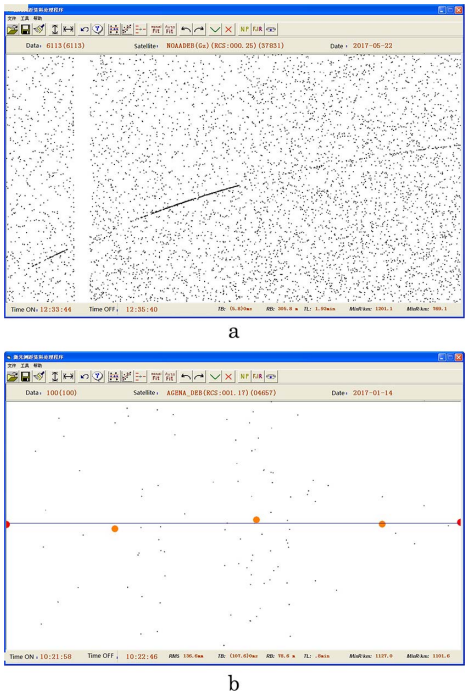

Fig. 5. Space debris laser ranging: a, smallest RCS, 0.25 m^2 (ID37831), and, b, best ranging precision, 13.68 cm (ID04657).

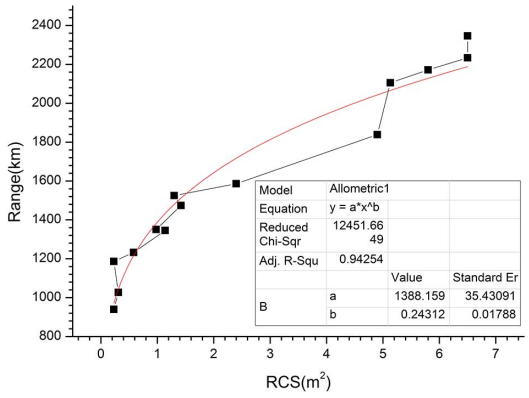

Fig. 6. Farthest measurement range of space debris RCS analysis.

where y is the farthest measurement range, and x is the RCS of the space debris. This was very consistent with the function of Eq. (3). We used this function to estimate and forecast the capability of our system.

The characteristics of space debris could be determined by laser ranging such as the spin rate[19,20]. Determining the space debris spin was very important in evaluating the space debris orbit or predicting when the space debris would fall to Earth. Laser ranging is the most advanced technology to measure self-spin. From Fig. 7(a), it is obvious that space debris ID14700 was spinning, named "Cosmos 1536 Rocket"; this debris had an orbit of 601.2×631 km, an orbital period of 97 min, and an inclination of 82.5°. The orbital period of its spin was 49 s. The spin parameters of space debris change under the influence of the forces and torques caused by Earth's gravitational and magnetic fields, as well as solar irradiation[19].

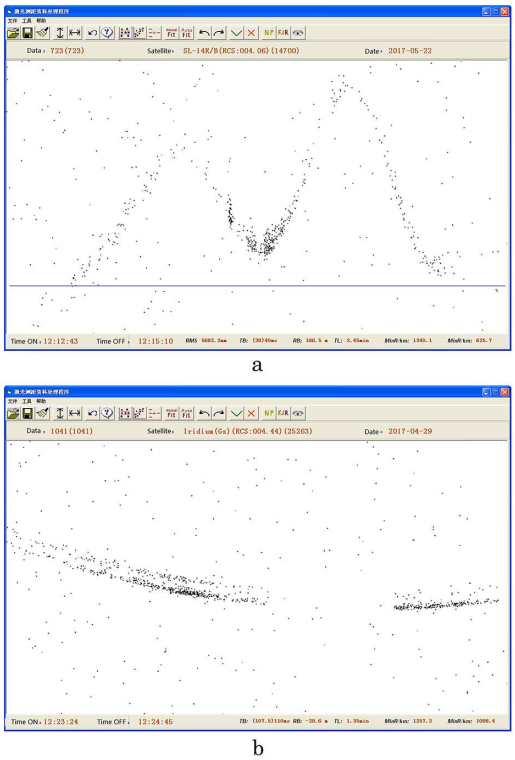

a

b

Fig. 7. Space debris characteristics: a, spin (ID14700) and, b, two reflective surfaces (ID25263).

It can be seen from Fig. 7(b) that space debris ID25263, named "Iridium 61," with an orbit of 758×762.1 km, an orbital period of 100 min, and an inclination of 86.4°, has two ranging lines, suggesting that there are possibly two reflective surfaces.

In summary, a proposed 60 W, 200 Hz, 532 nm, nanosecond slab, single-frequency green laser has been used to perform space debris laser ranging at SAO's 60 cm SLR system. In addition, many technologies were developed and renewed in the proposed SLR system. There were 174 passes of space debris measured in 2017, with the smallest RCS being 0.25 m^2 (ID37831) and the highest ranging precision at 13.6 cm (ID04657). All passes of space debris measured were analyzed, and the results show that the farthest measurement distance (R) and RCS (S) was fitted to $R = 1388.159S^{0.24312}$. This almost satisfies the radar equation and also shows the capability of the proposed SLR system using this laser. The spin of space debris was shown as well, which is very helpful in monitoring and studying space debris. A slab laser is easier to conduct heat treatment compared to other lasers, which is beneficial to the development of high-power, large-energy lasers and provides a better laser source for further measurement of space debris laser ranging. The accurate and reliable prediction of the orbit of space debris is crucially important for any effort in orbit conjunction analysis and for implementing collision-avoidance measures.

The authors thank the US Space Track Organization (www.space-track.org) and https://www.calsky.com/cs.cgi/Satellites for making available the two-line elements and names of cataloged objects, and the Shanghai Institute of Optics and Fine Mechanics for providing the laser. This work was supported by the National Natural Science Foundation of China (Nos. U1631240 and 11503068), the CAS Key Technology Talent Program, and the China Postdoctoral Science Foundation (Nos. BX201700270 and 2017M621562).

References

1. N. P. Khanolkar, N. Shukla, V. Kumar, and A. Vats, in *2017 International Conference on Infocom Technologies and Unmanned Systems* (2017), p. 854.
2. B. Esmiller, C. Jacquelard, H.-A. Eckel, and E. Wnuk, Appl. Opt. **53**, 145 (2014).
3. A. Tan, T. X. Zhang, and M. Dokhanian, Adv. Aerosp. Sci. Appl. **3**, 13 (2013).
4. J. C. Bennett, J. Sang, C. H. Smith, and K. Zhang, Adv. Space Res. **52**, 1876 (2013).
5. Q. Shi, Y. Zhang, K. Wang, C. Wang, and P. Zhao, Chin. Opt. Lett. **16**, 121401 (2018).
6. J. Sang and J. C. Bennett, Adv. Space Res. **54**, 119 (2014).
7. H. Hakima and M. R. Emami, Acta Astron. **144**, 225 (2018).

8. M. L. Long, Z. Zhang, Z. Chen, H. Zhang, H. Deng, Z. Wu, and W. Meng, Optik **171**, 833 (2018).
9. L. Xue, M. Li, L. Zhang, D. Zhai, Z. Li, L. Kang, Y. Li, H. Fu, M. Ming, S. Zhang, X. Tao, Y. Xiong, and P. Wu, Chin. Opt. Lett. **14**, 071201 (2016).
10. P. Lejba, T. Suchodolski, P. Michałek, J. Bartoszak, S. Schillak, and S. Zapasnik, Adv. Space Res. **61**, 2609 (2018).
11. G. Kirchner, F. Koidl, F. Friederich, I. Buske, U. Volker, and W. Riede, Adv. Space Res. **51**, 21 (2013).
12. Z. Wu, H. Zhang, W. Meng, P. Li, H. Deng, K. Tang, R. Ding, and Z. Zhang, Proc. SPIE **9796**, 97961E (2016).
13. G. Smith and M. J. Damzen, Opt. Express **15**, 6458 (2007).
14. J. Wang, J. Zhou, H. Zang, X. Zhu, and W. Chen, Chin. Opt. Lett. **8**, 670 (2010).
15. S. Li, X. Ma, H. Li, F. Li, X. Zhu, and W. Chen, Chin. Opt. Lett. **11**, 071402 (2013).
16. J. Ma, T. Lu, X. Zhu, X. Ma, S. Li, T. Zhou, and W. Chen, Chin. Opt. Lett. **16**, 081901 (2018).
17. Z.-P. Zhang, F.-M. Yang, H.-F. Zhang, Z.-B. Wu, J.-P. Chen, P. Li, and W.-D. Meng, Res. Astron. Astrophys. **12**, 212 (2012).
18. Z. Zhang, H. Zhang, M. Long, H. Deng, Z. Wu, and W. Meng, Optik **179**, 691 (2019).
19. D. Kucharski, G. Kirchner, F. Koidl, C. Fan, R. Carman, and C. Moore, IEEE Trans. Geosci. Remote Sens. **52**, 7651 (2014).
20. M. A. Steindorfer, G. Kirchner, F. Koidl, P. Wang, and D. Kucharski, in *IEEE International Conference on Environment and Electrical Engineering and IEEE Industrial and Commercial Power Systems Europe* (2017), p. 1.